Jurnal Kejuruteraan 38(1) 2026: 347-360
https://doi.org/10.17576/jkukm-2026-38(1)-31

Optimizing Palm Oil Recovery: CFD Insights into Sedimentation Tank Dynamics

Nur Tantiyani Ali Othman* & Seow Wai Kit

Department of Chemical and Process Engineering, Faculty of Engineering & Built Environment, Universiti Kebangsaan Malaysia, 43600, UKM Bangi Selangor, Malaysia

**Corresponding author: tantiyani@ukm.edu.com*

Received 18 June 2025, Received in revised form 13 September 2025
Accepted 13 October 2025, Available online 30 January 2026

ABSTRACT

The oil palm tree (Elaeis guineensis) is a major agricultural commodity in Malaysia, significantly contributing to the production of crude palm oil (CPO). Within the milling process, sedimentation is a critical stage that directly influences the quality of the final CPO product. Among the key parameters affecting sedimentation efficiency, fluid velocity plays a crucial role, particularly in controlling sludge blanket dynamics. This study investigates the optimal fluid velocity to enhance sedimentation performance, ensuring compliance with industry quality standards while minimizing the outflow cycle time of sedimentation tanks. To achieve this, Computational Fluid Dynamics (CFD) simulations were employed using COMSOL Multiphysics v6.3. A two-dimensional (2D) model of a sedimentation tank measuring 12.0 m in width and 4.0 m in height (total area: 48.0 m²) was developed. Inlet velocities ranging from 0.2 to 1.5 m/s were simulated using two turbulence models: k-ε and k-ω to assess their influence on flow behaviour, pressure distribution, and mass flux. Simulation results indicate that inlet velocities between 0.9 and 1.5 m/s yield optimal separation efficiency, minimizing oil losses to the sludge and maximizing oil recovery at the upper outlet. The study demonstrates the capability of CFD as a powerful tool for accurately simulating sedimentation tank performance, enabling real-time analysis and optimization of key operational parameters. This approach presents a cost-effective and practical solution for improving CPO quality and sedimentation efficiency in the palm oil mills, with the added benefits of reducing waste and enhancing overall process sustainability.

Keywords: Crude Palm Oil (CPO); sedimentation, Computational Fluid Dynamics (CFD); optimization

INTRODUCTION

The oil palm tree that is native to West and Central Africa belongs to the palm family *Arecaceae* and is a crucial agricultural resource especially in Malaysia and Indonesia. It is cultivated primarily for the extraction of palm oil that has become an integral part of the global economy. In its native regions, oil palm has been cultivated for centuries but its commercial expansion has seen it spread to other tropical countries such as Malaysia and Indonesia (Sustainable Palm Oil Choice 2018). Among these nations, Malaysia has become one of the world's leading producers of palm oil that contributes significantly to both country's agricultural economy and the global supply of Crude Palm Oil (CPO).

The oil palm tree belongs to the genus *Elaeis* which includes *E. guineensis* and *E. Oleifera*. Of these, *E. guineensis* is the predominant species used in plantation farming especially in Malaysia due to its higher yield and economic value (Chadwick 2017). The expansion of oil palm plantations in Malaysia has propelled the country to the second-largest global producer of palm oil. In the 2023/2024 period, Malaysia produced 19.71 million metric tons of palm oil and that was representing 26% of the world's total production (USDA 2024). This growing production is essential for supporting both local economies and global supply chains.

CPO often referred to as red palm oil is extracted from the mesocarp of palm fruits (Rey et al. 2023). It contains valuable minor components such as carotenoids,

tocopherols, tocotrienols, and phytosterols which contribute to its unique health benefits (Zou et al. 2012). Malaysia's production of CPO reached approximately 18.55 million metric tons in 2023 which marks a slight increase from the previous year's output (Siddharta 2024). The steady growth in CPO production underlines its importance in Malaysia's economy and its continued relevance in the global market.

The primary use of CPO is in the food industry where it serves as cooking oil and an ingredient in various packaged products. Palm oil is also extensively used in cosmetics, soaps and biofuels (WWF 2024). Beyond its widespread use, CPO is a preferred oil due to its stability, neutral taste and smooth texture. It is favored for its resistance to oxidative degradation which gives it a longer shelf life compared to other oils (Rey et al. 2023). The high demand for palm oil across various industries further highlights the need for efficient processing methods and quality control throughout the production process.

Fresh fruit bunches (FFB) are processed to extract CPO which is then refined into edible palm oil. In Malaysia, there are around 446 palm oil mills with 407 certified under the Malaysian Sustainable Palm Oil (MSPO) standard as of April 2024 (Ministry of Plantation and Commodities 2024). These mills span over 5.67 million hectares and cover about 17% of the country's total land area (Rajakal et al. 2024). The palm oil industry also contributes 2.7% to the national GDP with 90% of production being exported (IChemE 2022). In 2020, palm oil exports reached nearly 26,655 thousand metric tons which underscores industry's rank to Malaysia's foreign exchange earnings.

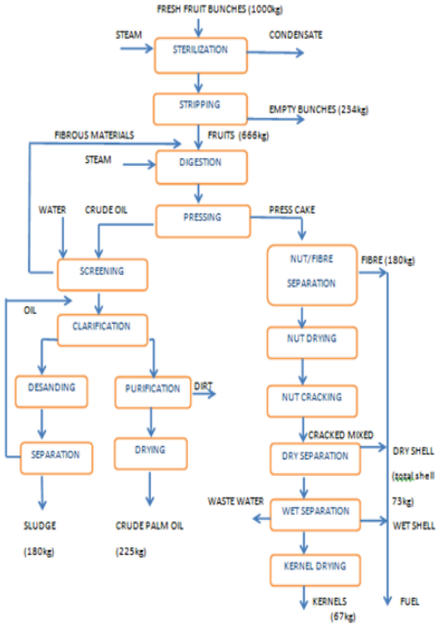

FIGURE 1. Palm Oil Milling (AOCS Lipid Library 2024)

Palm oil mills engage in some key processes to extract and refine CPO as shown in Figure 1 (AOCS Lipid Library 2024). The process includes sterilization, stripping, digestion, oil extraction, clarification, purification, kernel recovery and waste management. Among these, the clarification process is particularly important for determining the final quality of CPO. It involves separating oil from impurities and unwanted materials. The clarified CPO must meet specific quality standards including a maximum free fatty acid (FFA) content of 3.5%, a water content limit of 0.15% and an impurity level not exceeding 0.02% (Siregar et al. n.d.).

The clarification process plays a critical role in ensuring that CPO meets required quality standards. Through clarification, some factors influence the sedimentation process which are crucial for separating oil from solids and impurities. Key factors include particle size and shape, particle density, water temperature and the characteristics of the clarifier. The shape and size of particles affect how easily they settle, and the density of the particles determines their buoyancy and settling speed. In this process, temperature also plays a significant role. Studies have shown that elevated temperatures improve the settling efficiency by reducing the sludge blanket height and thus accelerating the settling process (Hayet et al. 2010). Increased temperature reduces the fluid's viscosity which allows particles to settle more quickly and efficiently. Thus, this will improve CPO quality (Kris & Ghawi 2008).

Fluid velocity is another critical factor in the clarification process. When the fluid velocity is too high, turbulence can occur which disrupts the settling of suspended particles. This leads to inefficiencies in the clarification process and results in poor oil quality and increased waste (Goula et al. 2008). To optimize the clarification process, it is essential to maintain an appropriate fluid velocity. Baffles and settlers are often used in clarifiers to reduce turbulence and stabilize the flow. They can help in ensuring a more efficient settling and improved CPO quality (Shahrokhi, Rostami, Md Said, et al. 2012).

A uniform temperature gradient is crucial for reducing oil viscosity and enhancing the separation of suspended particles and improving efficiency in sedimentation (Mohammad Fauzi et al. 2021). Areas with high velocity, typically near the inlet, exhibit turbulence that can disrupt the sedimentation process whereas low-velocity regions particularly at the bottom of the tank support sediment deposition. These velocity contours help to understand flow uniformity and sedimentation potential (Mohammad Fauzi et al. 2021). The consistent quality control of CPO during the sedimentation process faces significant challenges.

Ensuring consistent quality of CPO in the clarification process presents several challenges. One of the main issues

is the variation in fruit quality from the supplying estates which can significantly affect the oil extraction rate at the mill (Zulkefli et al. 2023). Also, inefficiencies in the clarification tank can lead to substantial oil losses. Research has indicated that the sludge stream contains a significant amount of oil with losses reaching up to 414 kg/hour in some cases (Kramanandita et al. 2014). Traditional monitoring methods, which often rely on manual sampling and measurements, are insufficient in optimizing the clarification process. These methods can take up to five days to verify the flow composition which leads to inefficiencies and waste (Ameran et al. 2017).

An additional key issue is reliance on conventional monitoring systems that often lack the accuracy and reliability needed to optimize operations, leading to inefficiencies and wastage. For instance, verifying flow composition using traditional sampling methods can take up to five days (Ameran et al. 2017). Traditional methods are inefficient because they rely heavily on manual sampling and laboratory testing which are time-consuming and prone to human error. These methods can take several days to deliver results in which they have the possibility of delaying crucial adjustments to the process. Additionally, they do not provide real-time data or detailed insight into internal tank dynamics and make it difficult to optimize sedimentation performance or prevent oil loss.

While advanced technologies such as CFD show potential, they remain underutilized and insufficiently explored as integrated solutions to these challenges. CFD offers significant advantages in understanding and optimizing the palm oil sedimentation process. It is a highly effective tool for analyzing fluid flow in complex systems. Through CFD simulations, fluid dynamics within sedimentation tanks can be modelled in detail, including velocity changes, flow direction and turbulence. This allows researchers to better understand the behavior of suspended solids during sedimentation. Moreover, CFD helps optimize operational parameters such as fluid velocity, temperature and tank geometry, ultimately reducing oil loss and improving sedimentation efficiency. Additionally, CFD simulations are cost-effective and time-saving alternatives to physical testing, reducing research costs and time. CFD's ability to predict the effects of changes in operational conditions provides an advantage in designing more efficient systems. Furthermore, this technology provides a more comprehensive two-dimensional view of the sedimentation process. CFD's predictive capabilities deliver a deeper understanding of fluid flow dynamics. This integration enhances control over the sedimentation process. An CFD-based monitoring system enables immediate adjustments and interventions based on current tank conditions while offering guidance for optimizing operational parameters.

Consequently, CPO quality can be better controlled, reducing oil loss to sludge streams. Moreover, CFD paves the way for developing more advanced and efficient sedimentation systems, adding significant value to palm oil mill operations. As for the lack of previous studies, this is likely due to limited awareness and technical expertise in CFD among palm oil industry stakeholders. Many mills prioritize operational continuity over technological innovation and there may be a perception that CFD is too complex or costly to implement. Furthermore, limited collaboration between academic researchers and industry players has contributed to the slow adoption of advanced simulation tools like CFD in this field.

The purpose of this study is to simulate the multiphase flow of a palm oil and water mixture within a sedimentation tank using Phase Transport Mixture Model under turbulent conditions which specifically employing k-ε and k-ω turbulence model. The simulation aims to analyze the behavior of oil and water phase separation within the geometry of the tank by considering realistic inlet and outlet flow rates. Furthermore, the study seeks to evaluate the effectiveness of the tank design in promoting optimal oil recovery while ensuring minimal oil loss through the bottom outlet, thereby assessing its efficiency in real-world operating conditions.

METHODOLOGY

The methodology utilizes several materials and tools for optimizing the palm oil clarification process. COMSOL Multiphysics software plays a crucial role in creating detailed models and defining the physics interfaces for CFD simulations. This software provides capabilities for geometry creation, meshing and solving the governing equations of fluid dynamics and electric fields which are essential in modelling the clarifier system. High-performance computational resources such as powerful computers or workstations are required to handle the demanding simulations and manage the extensive data generated during the analysis. These systems are equipped with advanced CPUs and sufficient RAM to ensure smooth operation of the simulations.

For defining material properties in the CFD model, physical parameters such as water, air and CPO are considered and defined as shown in Table 1. These properties are essential for simulating how different phases interact and impact capacitance measurements. In CFD model, fluid flow properties and boundary conditions are also vital to simulate the behavior of fluids and sedimentation in the clarifier. Meshing tools are employed to create refined mesh especially near critical areas. This ensures accurate

and reliable simulation results to facilitate precise analysis of fluid behavior and sedimentation processes.

TABLE 1. Global Definitions and Variables 1

Name	Value	Description
rho_c	1000 kg/m^3	Continuous Phase Density
mu_c	0.001 *Pa·s*	Continuous Phase Viscosity
rho_d	900 kg/m^3	Dispersed Phase Density
d_d	5E-5 μm	Dispersed Phase Particle Diameter
v_in	m/s	Inlet Velocity
v_out	m/s	Outlet Velocity
phid_in	kg/(m·s)	Inlet Volume Fraction of Dispersed Phase
qd_out	kg/(m·s)	Outlet Mass Flow Rate of Dispersed Phase

Final step, COMSOL's post-processing tools are used to visualize and analyze the simulation results. These tools generate flow patterns, velocity fields and sedimentation rates and this can offer valuable insights into the clarifier's performance and its influence on CPO quality. The findings will guide further optimization efforts for the system.

2D MODEL DEVELOPMENT OF SEDIMENTATION TANK

The CFD modelling for clarifiers begins by selecting 2D axisymmetric mode in COMSOL Multiphysics. In this study, a 2D model was selected to allow rapid numerical experimentation and parametric optimization while keeping computational cost manageable. Full 3D sedimentation tank modelling requires significantly higher mesh density and computational resources, which may limit the number of cases analyzed within the scope of this work. This mode simplifies simulation and reduces computational time while ensuring the accurate representation of fluid dynamics.

The geometry of the clarifier is constructed as a rectangle with dimensions tailored to the operational parameters of the palm oil mill. The clarifier's design is essential for simulating the fluid flow and sedimentation processes accurately. Figure 2 shows the sedimentation tank design with details geometry and dimension used for this research. The dimensions used were based on an actual industrial palm oil mill sedimentation tank, provided by Goula et al. 2008, which operates at maximum capacity of 10 tonnes/hour throughput. This ensured that the simulated flow conditions, residence time, and Reynolds numbers reflected real industrial practice rather than arbitrary laboratory scaling.

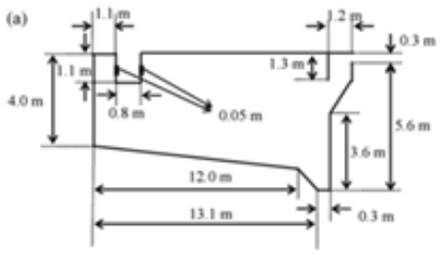

FIGURE 2. Sedimentation tank design with details geometry and dimension
Source: (Goula et al. 2008)

The fluid flow module in COMSOL is selected to model turbulent flow especially when the Reynolds number exceeds 4000 which is typical for this application. The *k-ε* turbulence model is used to capture the effects of turbulence which plays a crucial role in understanding the interaction between fluid flow and sedimentation. The realizable *k-ε* and SST *k-ω* models were selected because they are widely validated for sedimentation and multiphase separation in moderate-to-high Reynolds number flows (COMSOL 2025). The *k-ε* model performs well in bulk flow regions with fully developed turbulence, while *k-ω* SST is more accurate in near-wall and separation regions. Then, boundary conditions for inlet and outlet flows are defined to simulate realistic flow behavior. The model incorporates slip condition for the free surface and an axial symmetry condition for the clarifier's centerline.

Once the geometry is finalized, a mesh is generated to divide the domain into smaller elements for numerical computation. A finer mesh is created in areas where high flow gradients are expected, such as near the clarifier boundaries for accurate results. The computational domain was discretized using a structured triangular/quadrilateral mesh with 32, 000 number of elements, refined near the inlet, outlet, and sludge-oil-water interfaces to capture steep velocity and concentration gradients. A mesh independence test was conducted by comparing results at three mesh densities until changes in oil recovery efficiency were <1%. Velocity inlet at 0.2 m/s, pressure outlet atmospheric pressure, and no-slip walls for all tank surfaces. The sludge phase was represented by using a multiphase Euler–Euler approach with the mixture model, tracking oil, water, and sludge as separate phases with defined densities and viscosities.

The study type chosen for the simulation is time dependent as the system's behavior evolves over time. Transient models are essential for examining how flow and sedimentation processes fluctuate during the simulation. Once the study and solver settings are configured, the simulation is executed. The solver numerically solves the equations governing fluid flow, turbulence and sedimentation

based on the defined geometry and boundary conditions. After the simulation is completed, post-processing tools in COMSOL are used to visualize the results. These include flow patterns, velocity fields and turbulence intensities which help in understanding the dynamics of the fluid flow and sedimentation.

RESULT AND DISCUSSION

K-EPSILON (K-E) TURBULENCE MODEL

The k-epsilon (k-ε) turbulence model is a widely used two-equation model in CFD simulations for predicting turbulent flow. It calculates the turbulent kinetic energy (k) and rate of dissipation (epsilon) within the fluid flow. This model is suitable for steady flows and complex geometries, but it tends to be less accurate in regions near walls. Despite this limitation, it is commonly applied because it provides reliable results with relatively fast computation time (SimScale 2025a).

FLUID VELOCITY

The inlet velocity plays a crucial role in determining the flow pattern within the sedimentation tank. Changes in velocity can affect particle separation rates, vortex formation and the overall efficiency of the sedimentation process. If the velocity is too high, it may cause flow disturbances while a lower velocity might increase the fluid's residence time in the tank. Figure 3 shows the velocity magnitude of fluid flow within the sedimentation tank at a fixed simulation time of 43,200 seconds.

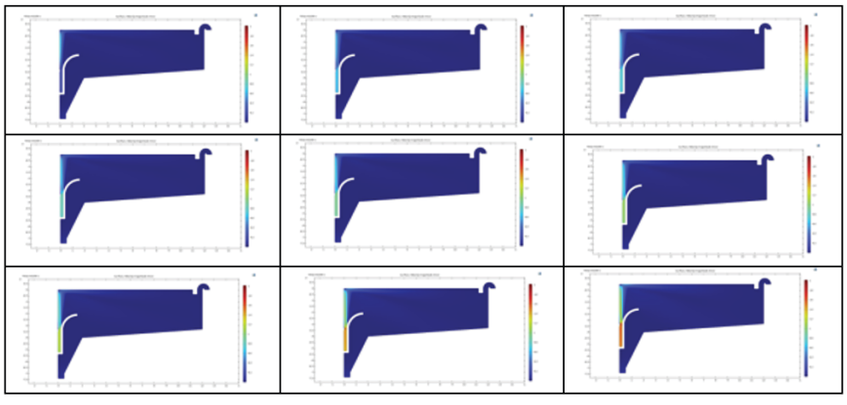

FIGURE 3. Overall results for the effect of inlet velocity on fluid in the sedimentation tank at a) 0.2 m/s, b) 0.6 m/s, c) 0.7 m/s, d) 0.8 m/s, e) 0.9 m/s, f) 1.0 m/s, g) 1.1 m/s, h) 1.4 m/s, i) 1.5 m/s

Each figure represents a different inlet velocity, namely 0.2, 0.6, 0.7, 0.8, 0.9, 1.0, 1.1, 1.4 and 1.5 m/s. The main difference between all these figures lies in how far and how fast the fluid travels within the tank. In general, as the inlet velocity increases, the fluid flows faster and reaches farther areas inside the sedimentation tank.

At an inlet flowrate of 0.2 m/s, the maximum velocity before the baffle was 0.6662 m/s and it slightly increased to 0.7553 m/s after the baffle. When the flowrate increased to 0.6 m/s, the velocity before the baffle decreased to 0.5707 m/s but rose after the baffle to 0.7938 m/s. At 0.7 m/s, the maximum velocity before the baffle increased to 0.9295 m/s but interestingly, it dropped to 0.5925 m/s after the baffle. For inlet flowrates of 0.8 and 0.9 m/s, the maximum velocity before the baffle continued to rise to 1.0656 m/s and 1.2016 m/s respectively while the post-baffle velocities were 0.6313 and 0.6780 m/s.

At 1.0 m/s, the velocity reached 1.3371 m/s before the baffle and 0.7340 m/s after it. As the flowrate increased further to 1.1 m/s, maximum velocity before the baffle became 1.4722 m/s and after the baffle, it was 0.7948 m/s. For higher flowrates of 1.4 and 1.5 m/s, the velocities before the baffle were 1.8805 m/s and 2.0181 m/s while the corresponding velocities after the baffle were 0.9962 and 1.0647 m/s. Overall, the data shows that fluid velocity generally increases with inlet flowrate and the baffle affects velocity differently depending on the flow regime, which is either increasing or decreasing it.

In Figure 3(a), which has the lowest inlet velocity of 0.2 m/s, the fluid flow is very slow. Most areas before the baffle appear in dark and light blue which indicates low velocity. The colour scale shows that the maximum velocity is only around 0.7 m/s. The flow does not travel far and quickly loses speed once it enters the main area of the tank. This indicates that at low inlet velocities, the fluid lacks the energy needed to circulate through the entire system. In contrast, Figures 3(b) to Figure 3(i) with the inlet velocities ranging from 0.6 m/s to 1.5 m/s show stronger

fluid flows. This is evident from the presence of green (medium velocity) and orange or red colors (high velocity) near the inlet. Based on the colour scale, the maximum velocities in these cases range from 0.7 m/s to 2.0 m/s. The fluid flow travels farther and retains more energy. Some areas also exhibit vortices or backflow, especially near curved regions, indicating the presence of turbulent flow.

Also, from Figures 3(c) to 3(i), it shows the effectiveness of using baffles to reduce horizontal flow velocity and direct particles to the bottom of the tank. These baffles are designed to control fluid velocity and reduce turbulence, thereby improving sedimentation efficiency (Shahrokhi, Rostami, Said, et al. 2012). Observations show that the baffles successfully slow down flow from the inlet and reduce turbulence within the tank. Although the flow after the baffle is still relatively strong, the velocity ranges between 0.6 to 1.8 m/s, which is still below the maximum velocity. As a result, these areas are shown in green to yellow instead of orange and red. The red areas only appear in certain spots with the highest velocity, typically at sharp corners or the bottom of the tank where flow accelerates due to tank geometry.

Yet, in Figures 3(a) and 3(b), there is a significant increase in the velocity immediately after the inlet baffle. In these cases, the baffle acts as a narrow passage that accelerates the fluid as it passes through the constricted space (Harner & Smith 2008). This occurs because when inlet velocity is low, pressure tends to build up in that area. According to Bernoulli's principle in fluid mechanics, when fluid passes through a narrow space like a baffle, part of the pressure energy is converted into kinetic energy (velocity) which leads to an increase in fluid speed (Harner & Smith 2008). Therefore, under these conditions, the baffle can cause the flow to accelerate rather than decelerate.

Figure 4 shows the effect of inlet velocity on fluid behaviour in the sedimentation tank where at an inlet velocity of 0.2 m/s, the fluid enters the tank slowly but its velocity increases after passing the baffle. Meanwhile, at 0.6 m/s, the fluid also starts at a low velocity but the change in velocity after the baffle is minimal. This observation suggests that the baffle is not effective when the inlet velocity is low. However, when the inlet velocity is within the range of 0.7 m/s to 1.5 m/s, the fluid velocity after the baffle gradually increases in line with the inlet velocity. Nevertheless, the velocity after the baffle remains lower than the inlet velocity. This indicates that the baffle works more effectively at higher velocities by slowing down the flow and providing better control.

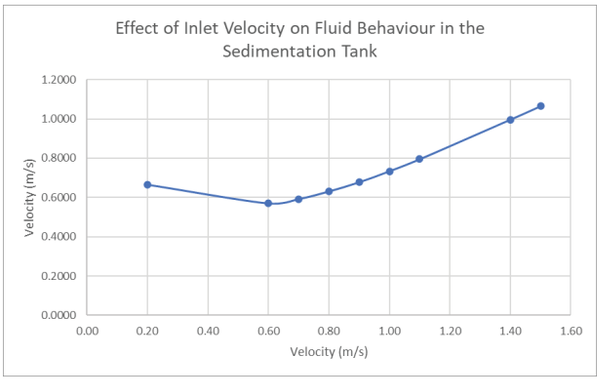

FIGURE 4. Effect of inlet velocity on fluid behaviour in the sedimentation tank

In conclusion, the simulation results show that fluid velocity in the sedimentation tank is influenced by both inlet velocity and the presence of internal baffles. Baffles are highly effective at controlling flow and reducing turbulence when the inlet velocity is high. However, if the inlet velocity is too low, the baffles may have the opposite effect by increasing velocity due to pressure buildup. Thus, to ensure optimal sedimentation performance, baffles should be used primarily when the inlet velocity is high, to ensure a more controlled flow and more effective particle settling.

PRESSURE DISTRIBUTION

The inlet velocity not only influences the fluid flow pattern but also has a direct impact on the pressure distribution within sedimentation tank. As velocity increases, pressure changes may occur due to stronger and more dynamic fluid motion. Uneven pressure can disrupt flow stability and reduce the effectiveness of particle separation. Therefore, understanding the relationship between velocity and pressure is crucial for designing and operating a more efficient sedimentation tank.

Figures 5(a) to 5(i) shows the pressure contours within the sedimentation tank for various inlet velocities, including 0.2, 0.6, 0.7, 0.8, 0.9, 1.0, 1.1, 1.4 and 1.5 m/s. Each figure shows how internal pressure changes spatially as fluid enters the tank at a specific speed. Despite the differences in inlet velocity, the pressure contour patterns across all figures appear relatively consistent throughout the tank.

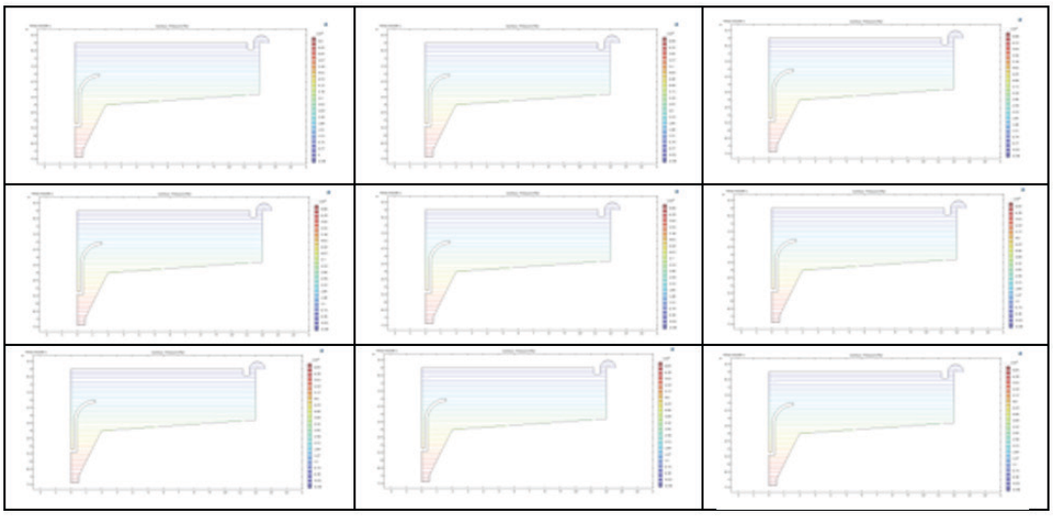

FIGURE 5. Overall results for the effect of inlet velocity on pressure in the sedimentation tank at a) 0.2 m/s, b) 0.6 m/s, c) 0.7 m/s, d) 0.8 m/s, e) 0.9 m/s, f) 1.0 m/s, g) 1.1 m/s, h) 1.4 m/s, i) 1.5 m/s

The pressure values at different inlet flowrates show a slight decreasing trend. At a flowrate of 0.2 m/s, the pressure was recorded at 6.8×10^4 Pa. As the flowrate increased to 0.6 m/s, the pressure dropped slightly to 6.69×10^4 Pa. This downward pattern continued with 6.68×10^4 Pa at 0.7 m/s, 6.67×10^4 Pa at 0.8 m/s and 6.66×10^4 Pa at both 0.9 m/s and 1.0 m/s. A further small drop to 6.65×10^4 Pa was observed at 1.1 m/s and the same pressure was maintained at higher flowrates of 1.4 m/s and 1.5 m/s. Although there is a slight decrease in pressure as the inlet flowrate increases, the overall change is minimal which indicates that the pressure remains relatively stable across the different flowrates.

At the base of the sedimentation tank, which is 4 meters deep, the pressure consists of atmospheric pressure plus the combined pressure from the layers of palm oil and water. In contrast, at the top of the tank, the pressure comes solely from the atmosphere. In the COMSOL simulation, the pressure contour colors clearly show a gradient from dark blue at the top (indicating low pressure) to dark red at the bottom (indicating high pressure). It is visually confirming the pressure increase with depth.

Although turbulence is introduced as the inlet velocity increases, its impact on the pressure distribution is minimal due to the presence of the baffle. The baffle helps stabilize the flow, reduce major disturbances and maintain a smooth pressure profile. While theoretically, stronger turbulence can shift pressure peaks earlier in the system (Haan et al. 1998), in this sedimentation tank case, the effect is negligible because the flow remains well-controlled.

Furthermore, pressure in a fluid is closely related to the force of gravity. This relationship can be observed through the behavior of fluids under gravitational influence. Gravity pulls fluid particles downward in which causing the lower layers of the fluid to support the weight of the fluid above. As a result, the deeper the fluid, the higher the pressure. This phenomenon is evident in various situations such as water in a lake or air in the atmosphere. In summary, pressure in a fluid increase with depth due to gravity as the weight of the fluid above presses downward and creates pressure at every point within the fluid (BBC Bitesize 2025).

Overall, the simulation indicates that pressure distribution in the sedimentation tank is mainly governed by hydrostatic effects. It shows that pressure increases almost linearly with depth and is only slightly influenced by changes in inlet velocity. Although higher inlet velocity may introduce minor turbulence, the presence of baffles helps maintain a stable pressure profile with significant differences only occurring between upper layer (low pressure) and the tank bottom (high pressure). Hence, a tank design with effective baffles can preserve pressure stability across varying inlet velocities for ensuring consistent separation performance.

MASS FLUX

The inlet velocity has a significant impact on mass flux within the sedimentation tank. Mass flux refers to the rate at which fluid mass flows through a specific area over a given period. As the inlet velocity increases, the amount of mass flowing through the system also changes. In a sedimentation tank system, these velocity changes can affect both the phase separation efficiency and the stability of fluid flow. Therefore, understanding the relationship between inlet velocity and mass flux is crucial to ensure more effective tank design and operation.

Figures 6(a) to 6(i) represent the mass flux of the dispersed phase at the inlet and outlets of the sedimentation tank across different inlet velocities, namely 0.2, 0.6, 0.7, 0.8, 0.9, 1.0, 1.1, 1.4 and 1.5 m/s. By analyzing these mass flux graphs, one can understand how fluid flow evolves over time and how it is distributed between the two outlet channels. The mass flux at Outlet 2 shows a generally increasing trend as the inlet flowrate rises. At the lowest flowrate of 0.2 m/s, the mass flux was recorded as negative with a value of -3.624 kg/s which is possibly due to reverse or recirculating flow. When the inlet flowrate increased to 0.6 m/s, the mass flux sharply increased to 13.010 kg/s. This upward trend continued with values of 18.210 kg/s at 0.7 m/s, 23.737 kg/s at 0.8 m/s and 29.170 kg/s at 0.9 m/s. The increase remained consistent with 34.620 kg/s at 1.0 m/s and 40.050 kg/s at 1.1 m/s. At even higher inlet flowrates of 1.4 m/s and 1.5 m/s, the mass flux jumped further to 56.519 kg/s and peaked at 61.464 kg/s respectively. Overall, this trend indicates that the mass flux at the outlet increases steadily with inlet flowrate especially after overcoming the initial anomaly at 0.2 m/s.

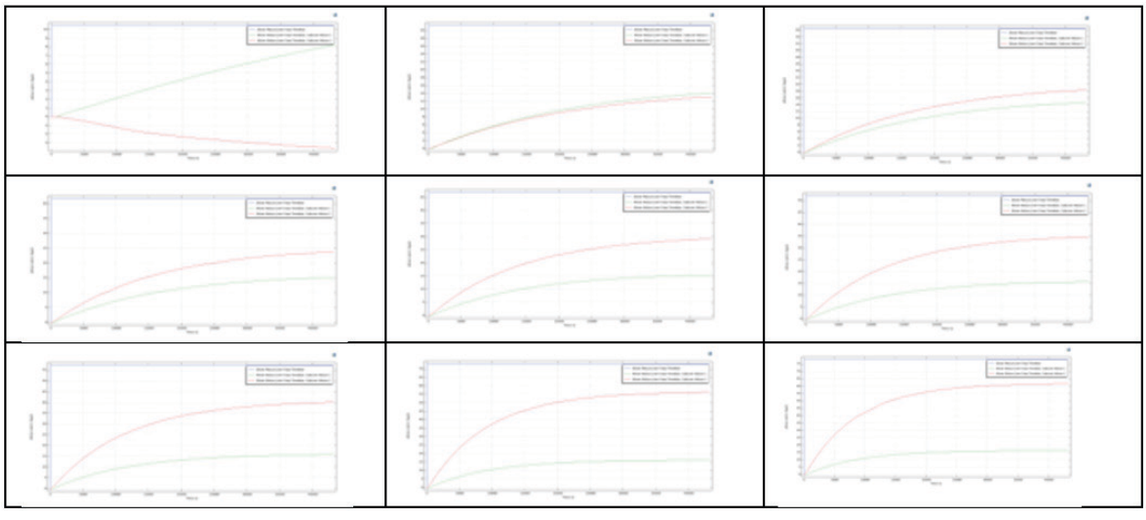

FIGURE 6. Overall results for the effect of inlet velocity on mass flux in the sedimentation tank at a) 0.2 m/s, b) 0.6 m/s, c) 0.7 m/s, d) 0.8 m/s, e) 0.9 m/s, f) 1.0 m/s, g) 1.1 m/s, h) 1.4 m/s, i) 1.5 m/s

Figure 7 presents the graph for the effect of inlet velocity on mass flux in the tank. It is showing that as inlet velocity increases, the mass flux at the tank outlets also rises. This observation is essential for evaluating system stability and the effectiveness of the tank design in handling flow at different speeds.

Since most of the graphs show similar trends, only two cases which are selected for comparison to better highlight the differences. In both scenarios, the outlet mass flow increases gradually throughout the simulation. The blue line which represents the inlet mass flux remains constant while the green and red lines representing Outlet 1 and Outlet 2 increase and approach a stable value, though not identical. This suggests that the system eventually reaches a dynamic equilibrium where the flow is distributed between both outlets. For the 0.6 m/s case, the inlet mass flux stabilizes around 31 kg/s while Outlet 1 and Outlet 2 stabilize at approximately 14 kg/s and 13 kg/s respectively.

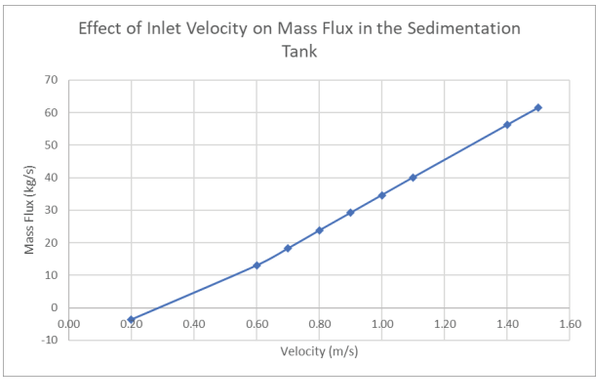

FIGURE 7. Effect of inlet velocity on mass flux in the sedimentation tank

As compared to both velocities, it becomes clear that the difference between Outlet 1 and Outlet 2 is more significant at 1.5 m/s. This is because a higher inlet velocity introduces a greater amount of fluid mass into the tank. At high velocities, any imbalance in outlet resistance or tank design becomes more pronounced. In this case, Outlet 2 (red line) becomes more dominant while Outlet 1 (green

line) receives less flow. Although this imbalance is also present in the 0.6 m/s case, it is less significant, which is indicating a more balanced distribution at moderate velocities. Due to this imbalance in mass flux separation, more palm oil is collected at Outlet 2 than at Outlet 1. This shows that the separation efficiency improves as the inlet velocity increases. This might be due to the higher pushing force at higher velocities which drives the oil horizontally across the tank and allows more of it to be captured at Outlet 2. However, the increased velocity also pushes more water toward Outlet 2 and is resulting in a higher water collection there as well.

At the lowest velocity of 0.2 m/s, the trend is drastically different. The low inlet mass flow means very little fluid enters the system. Initially, Outlet 2 shows a positive value, but it later decreases to the negative which indicates a backflow. Meanwhile, the flow at Outlet 1 gradually increases and it is suggesting instability and imbalance in the system. With such low flow energy, the system pressure may be insufficient to even distribute fluid to both outlets. This will be causing one outlet to draw fluid back into the system due to pressure or momentum differences. This scenario is known as back pressure, occurs when downstream water pressure becomes greater than the supply pressure and is potentially disrupting the flow and even reversing it in some cases (Charles County 2025).

In summary, the flow pattern and mass flux separation in the sedimentation tank are directly influenced by inlet velocity. At moderate velocity (e.g., 0.6 m/s), the distribution between Outlet 1 and 2 is more balanced and it indicates stable system performance. However, at high velocity like 1.5 m/s, separation becomes more efficient with more oil collected at Outlet 2 though more water also exits through the same outlet. This shows that higher velocities provide strong driving force to transport oil to the far end of the tank but also carry water along. Therefore, the use of baffles is highly recommended at high inlet velocities as they help manage and control the flow more effectively (Shahrokhi, Rostami, Md Said, et al. 2012). On the other hand, at very low velocities such as 0.2 m/s, the system becomes unstable, and this leads to backflow due to insufficient pressure. Hence, inlet velocity must be controlled within an optimal range to ensure effective phase separation without compromising system stability.

FLUID BEHAVIOR IN SEDIMENTATION TANK

The inlet velocity plays a key role in shaping the phase flow contours within the sedimentation tank. These contours illustrate the direction and flow patterns between fluid phases such as oil and water inside the tank. Changes in inlet velocity can influence how these two phases move, mix or separate from one another. A velocity that is too high may create strong turbulence while a lower velocity supports stable flow and more efficient phase separation. Therefore, studying the effects of inlet velocity is important for understanding phase flow behavior and improving the performance of the sedimentation system.

Figures 8(a) to 8(b) show how different inlet velocities such as 0.2, 0.6, 0.7, 0.8, 0.9, 1.0, 1.1, 1.4 and 1.5 m/s affect flow behavior, both dispersed and continuous phases, inside the sedimentation tank. As the inlet velocity increases, the way the fluid moves and spreads in tank changes noticeably. As the inlet flowrate increases, the volume fraction at Outlet 2 shows a clear and steady rise. At a low inlet flowrate of 0.2 m/s, the volume fraction was 0.0000 which indicates no presence of the dispersed phase.

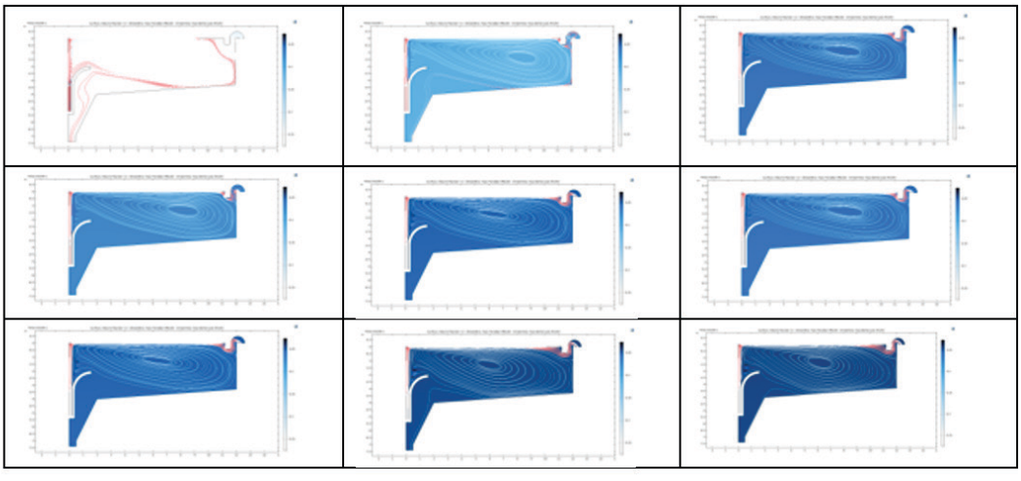

FIGURE 8. Overall results for the effect of inlet velocity on phase flow contour in the sedimentation tank at a) 0.2 m/s, b) 0.6 m/s, c) 0.7 m/s, d) 0.8 m/s, e) 0.9 m/s, f) 1.0 m/s, g) 1.1 m/s, h) 1.4 m/s, i) 1.5 m/s

When the inlet flowrate increased to 0.6 m/s, the volume fraction jumped significantly to 0.4005. This upward trend continued with values of 0.4176 at 0.7 m/s, 0.4298 at 0.8 m/s and 0.4386 at 0.9 m/s. The volume fraction kept increasing at higher flowrates until it reaches 0.4448 at 1.0 m/s, 0.4493 at 1.1 m/s, 0.4562 at 1.4 m/s and slightly higher at 0.4573 for 1.5 m/s. Overall, this pattern shows a strong positive correlation between inlet flowrate and volume fraction and is suggesting that more of the dispersed phase successfully exits through Outlet 2 as the flowrate increases.

At the lowest inlet velocity of 0.2 m/s, the fluid flows very slowly and mostly stay near the inlet zone. This low speed limits the movement of the dispersed phase and is making it hard for the oil to spread throughout the tank. As a result, most of the oil is lost through Outlet 1. In addition, because there is not enough energy to push the fluid forward, back-flows or stagnant pockets may occur. Weak circulation and poor phase separation show that such a low velocity is unsuitable for effective settling.

When the inlet velocity is raised to a moderate range between 0.6 and 1.1 m/s, the flow in the tank improves. The fluid can travel farther and recirculate more effectively. This allows both oil and water to spread over a wider area. This helps improve separation efficiency. At this stage the baffle plays a crucial role by guiding the flow direction and reducing excessive horizontal motion. As a result, turbulence can be controlled, and the flow becomes more stable. For inlet velocities between 0.8 m/s and 1.5 m/s, most of the palm oil is successfully collected at Outlet 2 and a reasonable amount of water is also found there. Meanwhile, at lower velocities such as 0.6 and 0.7 m/s only small amounts of oil which are 14 kg/s and 15 kg/s respectively are detected at Outlet 1.

At high inlet velocities, such as 1.4 and 1.5 m/s, the fluid travels deeper into the tank, allowing the dispersed phase to reach the bottom of the settling zone. However, the high speed near the entrance creates strong local turbulence. This excess kinetic energy can resuspend particles that have already settled, reducing separation efficiency. The flow becomes difficult to control, and the movement pattern grows more complex. Although most oil is still collected at Outlet 2, the strong inlet jet also forces a large amount of water out through the same outlet which may be undesirable.

Figure 9 shows how changes in inlet velocity affect the volume fractions of oil and water at Outlet 2. Two clear trends appear which are as inlet velocity rises, the oil fraction steadily increases while the water fraction decreases. At the lowest velocity of 0.2 m/s, the mixture is almost entirely water, and the blue oil curve starts near zero fraction while the orange water curve is high around 0.75. This indicates that the gentle flow lacks enough energy to lift and transport oil droplets to the observation point so very little oil is detected there. When the velocity reaches 0.6 m/s, a sharp change occurs. The oil fraction jumps to about 0.40 and the water fraction falls to around 0.60. At this moderate speed, flow carries more momentum, encouraging oil droplets to coalesce and rise, thus increasing the observed oil content. At the same time, the stronger jet pushes some water out of the sampling zone and lowers its fraction. Beyond 0.6 m/s, as the inlet velocity climbs from 0.7 to 1.5 m/s, the rise in oil fraction slows. The blue line creeps upward and finally level off near 0.45 to 0.46, while the orange water line slowly declines and stabilizes around 0.53 to 0.54. This plateau suggests that once the flow passes a certain threshold, further increases offer little benefit as the oil-water separation is already near its maximum practical efficiency. Excessive turbulence can even hinder further improvement by re-entraining separated droplets although this effect is minor within the tested range.

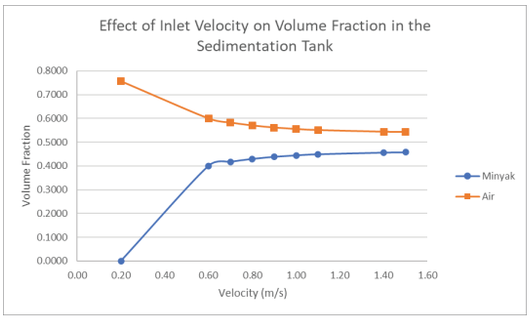

FIGURE 9. Effect of inlet velocity on volume fraction in the sedimentation tank

Besides inlet velocity, the simulation results also show behavioral differences between the dispersed and continuous phases. Raw palm oil, with an approximate density of 900 kg/m³, tends to float near the top because of its lower density. Water, with a density of 1000 kg/m³, spreads more evenly throughout the tank. This density difference supports natural gravitational separation: denser fluid moves downward, while lighter fluid rises (Jayakrishnan & Chakravarthy 2017). At an optimal inlet velocity, both oil and water can form stable layers, improving efficiency.

The baffle is an important component throughout the simulation. Its main function is to slow the fluid's horizontal speed after it enters the tank which helps vertical settling of particles more effectively. It also reduces turbulence intensity, especially at high inlet velocities and guides both phases to spread more evenly in the settling zone. Although at very low velocities, baffles may cause a slight speed increase due to the Bernoulli effect, overall, it remains effective in stabilizing the flow. The presence

of the baffle is particularly valuable at moderate to high inlet velocities, where uncontrolled turbulence could reduce process performance.

COMPARISON BETWEEN K-E AND K-Ω TURBULENCE MODELS

The *k-ε* and *k-ω* turbulence models are two commonly used approaches in CFD simulations to represent complex fluid flows. Both models share a similar fundamental concept which involves using two equations to calculate turbulent kinetic energy (*k*) along with an additional variable which is either epsilon in *k-ε* model or omega in the k-ω model. Although they are based on the same core principles, these models differ in terms of accuracy, sensitivity to near-wall flow and simulation stability. Therefore, this section will clearly outline and compare the key differences between two models.

DIFFERENCES IN CHARACTERISTICS OF TURBULENCE MODELS

Firstly, in terms of performance near wall regions, the *k-ω* model demonstrates a clear advantage because it can estimate flow behavior close to walls more accurately. This is due to its ability to directly model the viscous sublayer without the need for additional wall functions (CFD Online 2021). In contrast, the *k-ε* model requires special wall functions or a very fine mesh, where y^+ value must be less than 5 to achieve accurate results (SimScale 2025a). Next, in flow conditions involving pressure gradients, the *k-ω* model tends to provide more precise estimations. However, it may sometimes overpredict flow separation regions. On the other hand, the *k-ε* model often yields less accurate predictions and can sometimes completely fail to handle such flow scenarios. Lastly, in transitional flows that is, flows transitioning from laminar to turbulent, the *k-ω* model can predict this transition although it may occasionally predict the transition prematurely (SimScale 2025b). In contrast, the *k-ε* model is unable to model this type of flow transition effectively (SimScale 2025a).

RESULT ACCURACY

The *k-ω* turbulence model is more suitable than the *k-ε* model when simulating real-world fluid flow problems, especially in complex geometries like sedimentation tanks. This is because *k-ω* considers detailed flow characteristics in three critical areas such as near-wall performance, pressure gradient sensitivity and transition flow handling. Due to its sensitivity to these factors, k-ω can provide a more detailed and physically realistic representation of fluid behavior. This is evident when compared as shown in Figure 10 that represents the flow of fluid for *k-ε* and *k-ω*.

It shows the simulation offers clearer visualization of the flow distribution and captures more refined patterns of circulation and turbulence within the tank. Also, the simulation coverage for *k-ω* is broader which indicates that the *k-ω* model resolves the fluid field with greater detail than the *k-ε* model. Thus, it can be concluded that *k-ω* offers well alignment with real-world conditions, especially when high-fidelity results are desirable for performance evaluation in the systems that are influenced by wall interactions, pressure variation and transitional flow behavior.

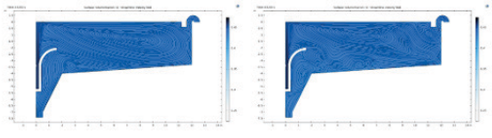

FIGURE 10. Flow Contour in *k-ε* and *k-ω*

Besides, although the mass flux curves of the *k-ε* and *k-ω* models appear similar, some subtle differences can still be observed. One key observation is that the *k-ω* mass flux curve appears less smooth, with slight fluctuations, compared to the more consistent curve of the *k-ε* model as shown in Figure 11. This may be due to the inherent nature of the *k-ω* model, which is more sensitive to near-wall flow behavior and transitional flow. Thus, it responds more actively to small-scale disturbances in fluid (SimScale 2025b). Hence, the outcomes produced by the *k-ω* model can be considered more realistic compared to those from the *k-ε* model.

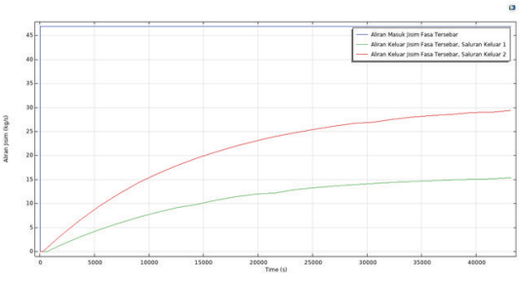

FIGURE 11. Mass flux curve for k-ω

PHASE SEPARATION EFFICIENCY BASED ON INLET VELOCITY

The simulation results indicate that both *k-ε* and *k-ω* turbulence models demonstrate similar efficiency values within the inlet velocity range of 0.6 to 0.9 m/s where the

separation efficiency remains around 40-60% as shown in Figure 12. However, to confidently determine whether both models truly perform at the same level or if one offers superior efficiency, a broader range of inlet velocities and more comprehensive data would be required. It is also important to highlight that the current efficiency values may not accurately reflect real-world performance. This is likely due to the simplified nature of the simulation setup. Achieving more realistic and reliable outcomes would require further refinement in several aspects, including geometry, mesh resolution, physical modelling and the overall study configuration within the COMSOL Multiphysics environment. Due to time limitations, the project was only able to simulate four cases using the *k-ω* model. Simulations were run using both turbulence models. The *k–ω* SST model predicted slightly lower oil recovery 65% vs 80% for *k–ε* and higher sludge carryover 34% vs 26%, likely due to its better near-wall resolution and improved prediction of inlet feed. As a result, the comparison between these two turbulence models remains limited and cannot be considered fully conclusive.

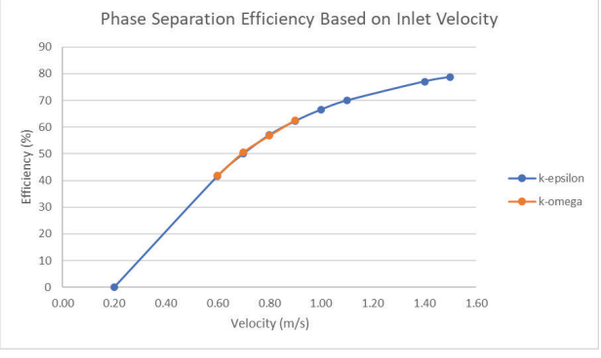

FIGURE 12. Phase separation efficiency based on inlet velocity

For validate this simulation result, until now, there are no new experimental campaign was conducted within the timeframe of this study. However, the simulation results were compared to historical performance data from the same palm oil mill. The predicted oil recovery differed by less than 5.5% from the average measured plant recovery, indicating that the numerical model is representative. Yet, the key trends observed such as the influence of inlet velocity, sludge withdrawal rate, and baffle position on separation efficiency are consistent with findings previously reported for other edible oil and wastewater sedimentation systems.

CONCLUSION

This study successfully met its objectives by using Computational Fluid Dynamics (CFD) to optimize sedimentation tank performance in crude palm oil (CPO) processing. The 2D tank design simulated in COMSOL improved phase separation efficiency, while comparisons of *k-ε* and *k-ω* turbulence models revealed that fluid velocity between 0.9 and 1.1 m/s yielded the best oil-water separation. Visual analyses confirmed the critical role of flow conditions on separation behavior. The findings demonstrate that CFD offers a cost-effective and accurate approach for optimizing tank design and operations without requiring physical trials. This contributes to higher recovery of oil, reduced waste, and improved economic sustainability in palm oil mills. Furthermore, the study aligns with SDG 9 by promoting innovative and efficient industrial practices through digital simulation technology. Overall, CFD proves to be a powerful tool for enhancing CPO quality, operational efficiency, and sustainability.

ACKNOWLEDGEMENT

This research is fully supported by FRGS grant, FRGS/1/2024/TK05/UKM/02/4 and GUP-2024-061. The authors fully acknowledged Ministry of Higher Education (MOHE) and Universiti Kebangsaan Malaysia for the approved fund which makes this important research viable and effective.

DECLARATION OF COMPETING INTEREST

None.

REFERENCES

Ameran, H.L.M., Mohamad, E.J., Rahim, R.A., Rashid, W.N.A. & Mansor, Z. 2017. Design of crude palm oil monitoring system using electrical capacitance tomography: A conceptual framework. *International Journal on Advanced Science, Engineering and Information Technology* 7(4): 1374–1380. https://www.researchgate.net/publication/319403972_Design_of_Crude_Palm_Oil_Monitoring_System_using_Electrical_Capacitance_Tomography_A_Conceptual_Framework [11 December 2024].

AOCS Lipid Library. 2024. Palm oil. *AOCS Lipid Library*. https://lipidlibrary.aocs.org/edible-oil-processing/palm-oil [8 December 2024].

Atoyebi, E.O., Oyejide, A.J., Dele-Afolabi, T.T., Mohamed Ariff, A.H. & Ojo-Kupoluyi, O.J. 2024. Scaffold modeling advancement in biomaterials

application. *Comprehensive Materials Processing*: 56–71.

BBC Bitesize. 2025. Pressure in a liquid – Higher – Pressure in fluids – AQA – GCSE Physics (Single Science) revision. *BBC Bitesize*. https://www.bbc.co.uk/bitesize/guides/z93dxfr/revision/2 [13 July 2025].

Brentwood. 2017. Rectangular vs. circular clarifiers: Choosing the best option. *Brentwood Industries*. https://www.brentwoodindustries.com/resources/learning-center/water-wastewater/rectangular-vs-circular-clarifiers-what-is-the-best-option/ [11 January 2025].

BYJU'S. 2025. What is hydrostatic pressure? *BYJU'S*. https://byjus.com/physics/hydrostatic-pressure/ [15 June 2025].

CFD Online. 2021. Near-wall treatment for k-omega models – CFD-Wiki, the free CFD reference. *CFD Online*. https://www.cfd-online.com/Wiki/Near-wall_treatment_for_k-omega_models [18 June 2025].

Chadwick, R. 2017. Ethics and genetically modified crops. In Thomas, B. (ed.). *Encyclopedia of Applied Plant Sciences* 1: 8–12. http://www.sciencedirect.com:5070/referencework/9780123948083/encyclopedia-of-applied-plant-sciences [25 November 2023].

Charles County, M. 2025. Backsiphonage and backpressure. *Charles County, MD*. https://www.charlescountymd.gov/services/public-works-utilities/cross-connection-control-program/backsiphonage-and-backpressure [15 June 2025].

Chukwulozie, O., Segun, O., Lekwuwa, C. & Chiagoro, U. 2018. Design of sewage treatment plant for CBN housing estate Trans-Ekulu Enugu Nigeria. *Advances in Research* 13(3): 1–18.

COMSOL. 2025a. Contaminant-removal from wastewater in a secondary clarifier by sedimentation. *COMSOL Model Gallery*. https://www.comsol.com/model/contaminant-removal-from-wastewater-in-a-secondary-clarifier-by-sedimentation-2163 [16 June 2025].

COMSOL. 2025b. The k-ε turbulence model. *COMSOL Documentation*. https://doc.comsol.com/5.5/doc/com.comsol.help.cfd/cfd_ug_fluidflow_single.06.088.html [15 July 2025].

COMSOL. 2025c. The k-ω turbulence model. *COMSOL Documentation*. https://doc.comsol.com/5.5/doc/com.comsol.help.cfd/cfd_ug_fluidflow_single.06.090.html [15 July 2025].

Fauzi, A.H.M. 2021. *IOP Conference Series: Earth and Environmental Science*. IOP Science.

Goula, A.M., Kostoglou, M., Karapantsios, T.D. & Zouboulis, A.I. 2008. A CFD methodology for the design of sedimentation tanks in potable water treatment: Case study: The influence of a feed flow control baffle. *Chemical Engineering Journal* 140(1–3): 110–121.

Haan, F.L., Kareem, A. & Szewczyk, A.A. 1998. The effects of turbulence on the pressure distribution around a rectangular prism. *Journal of Wind Engineering and Industrial Aerodynamics* 77–78: 381–392. https://www.sciencedirect.com/science/article/pii/S0167610598001585 [15 June 2025].

Harner, J.P. & Smith, J.F. 2008. "Let it flow, let it flow": Moving air into the freestall space.

Hayet, C., Hédi, S., Sami, A., Ghada, J. & Mariem, M. 2010. Temperature effect on settling velocity of activated sludge. *ICBEE 2010 – 2nd International Conference on Chemical, Biological and Environmental Engineering, Proceedings*: 290–292. https://www.researchgate.net/publication/241177077_Temperature_effect_on_settling_velocity_of_activated_sludge [10 January 2025].

IChemE. 2022. International Palm Oil Sustainability Conference. *IChemE*. https://www.icheme.org/media/19096/iposc-infographics-2.pdf [8 January 2025].

Jayakrishnan, J.S. & Chakravarthy, C.P. 2017. Flux bounded tungsten inert gas welding for enhanced weld performance – A review. *Journal of Manufacturing Processes* 28: 116–130. https://www.sciencedirect.com/science/article/abs/pii/S1526612517301342 [15 June 2025].

Kramanandita, R., Bantacut, T., Romli, M. & Makmoen, M. 2014. Utilization of palm oil mills wastes as source of energy and water in the production process of crude palm oil. *ResearchGate*. https://www.researchgate.net/publication/280534556_Utilization_of_Palm_Oil_Mills_Wastes_as_Source_of_Energy_and_Water_in_the_Production_Process_of_Crude_Palm_Oil#pf3 [11 December 2024].

Kris, J. & Ghawi, A.H. 2008. Study the effect of temperature on sedimentation tanks performance. *ResearchGate*. https://www.researchgate.net/publication/312025431_Study_the_Effect_of_Temperature_on_Sedimentation_Tanks_Performance [8 December 2024].

Ministry of Plantation and Commodities. 2024. SAWIT: MSPO certification achieves 87.4% coverage of Malaysian palm oil plantations. *Laman Web Rasmi KPK*. https://www.kpk.gov.my/kpk/en/palm-oil-news/sawit-mspo-certification-achieves-87-4-coverage-of-malaysian-palm-oil-plantations [8 January 2025].

Mohammad Fauzi, A.H., Saifuddin, M.N.A.A., Kasim, F.H. & Zakaria, Z.Y. 2021. Simulation of crude palm oil dilution and clarification in a palm oil mill using computational fluid dynamics: Grid dependency and parametric studies. *IOP Conference Series: Earth and Environmental Science* 765(1). https://www.researchgate.net/publication/351831446_Simulation_of_crude_palm_oil_dilution_and_clarification_in_a_palm_oil_mill_using_computational_fluid_dynamics_Grid_dependency_and_parametric_studies [8 December 2024].

Rajakal, J.P., Ng, F.Y., Zulkifli, A., How, B.S., Sunarso, J., Ng, D.K.S. & Andiappan, V. 2024. Analysis of current state, gaps, and opportunities for technologies in the Malaysian oil palm estates and palm oil mills towards net-zero emissions. *Heliyon* 10(10): e30768.

Rey, F., Alves, E., Gaspar, L., Conceição, M. & Domingues, M.R. 2023. Oils as a source of bioactive lipids (olive oil, palm oil, fish oil). In *Bioactive Lipids*: 231–268.

Shahrokhi, M., Rostami, F., Md Said, M.A., Sabbagh Yazdi, S.R. & Syafalni. 2012. The effect of number of baffles on the improvement efficiency of primary sedimentation tanks. *Applied Mathematical Modelling* 36(8): 3725–3735.

Shahrokhi, M., Rostami, F., Said, M.A.M., Sabbagh-Yazdi, S.R., Syafalni, S. & Abdullah, R. 2012. The effect of baffle angle on primary sedimentation tank efficiency. 39(3): 293–303. https://doi.org/10.1139/l2012-002. [11 December 2024].

Siddharta, A. 2024. Malaysia: Crude palm oil production volume 2023. *Statista*. https://www.statista.com/statistics/794709/crude-palm-oil-production-volume-malaysia/ [8 January 2025].

SimScale. 2025a. k-epsilon turbulence model | Global settings | SimScale. *SimScale Documentation*. https://www.simscale.com/docs/simulation-setup/global-settings/k-epsilon/ [18 June 2025].

SimScale. 2025b. k-omega turbulence models | Global settings | SimScale. *SimScale Documentation*. https://www.simscale.com/docs/simulation-setup/global-settings/k-omega-sst/ [18 June 2025].

Siregar, K., Ishak, A. & Sinaga, H.A. t.th. Quality control of crude palm oil (CPO) using define, measure, analyze, improve, control (DMAIC) and fuzzy failure mode and effect analysis.

Styra, D. & Babout, L. 2010. Improvement of AC-based electrical capacitance tomography hardware. *ResearchGate*. https://www.researchgate.net/publication/228789576_Improvement_of_AC-based_Electrical_Capacitance_Tomography_Hardware [8 December 2024].

Sustainable Palm Oil Choice. 2018. Facts on palm oil. *Sustainable Palm Oil Choice*. https://www.sustainablepalmoilchoice.eu/facts-on-palm-oil/ [8 January 2025].

USDA. 2024. Palm oil. *USDA Foreign Agricultural Service*. Foreign Agricultural Service – U.S. Department of Agriculture. https://fas.usda.gov/data/production/commodity/4243000 [11 December 2024].

WWF. 2024. What is palm oil? Facts about the palm oil industry. *WWF*. https://www.worldwildlife.org/industries/palm-oil [8 January 2025].

Zou, Y., Jiang, Y., Yang, T., Hu, P. & Xu, X. 2012. Minor constituents of palm oil: Characterization, processing, and application. In *Palm Oil: Production, Processing, Characterization, and Uses*: 471–526.

Zulkefli, F., Othman, N., Syahlan, S., Zaini, M.R. & Bakar, M.A. 2023. Fresh fruit bunch quality and oil losses in milling processes as factors that affect the extraction rate of palm oil. *International Journal of Agriculture, Forestry and Plantation*. https://ijafp.org/wp-content/uploads/2017/10/PL-24.pdf [11 December 2024].